131

Egypt. J. Chem. **Vol. 65,** No. 2 pp. 609 - 622 (2022)

Egyptian Journal of Chemistry

http://ejchem.journals.ekb.eg/

Therapeutic Efficacy of Kumquat-Loaded Chitosan Nanoparticles against Toxoplasmosis in mice model

Wafaa Fayez Abd El-Hamed[a], Nahed Samy Yousef[b], Ahmed A. Abd-Rabou[c*], Zainab Abdul-Wahhab Salem[d]

[a].Biological and Environmental Sciences Dept., Faculty of Home Economics, Al-Azhar University, Egypt
[b]Food Science and Technology Dept., Faculty of Home Economics, Al-Azhar University, Egypt
[c]Hormones Department, Medical Research and Clinical Institute, and Stem Cell Laboratory, Center of Excellence for Advanced Science, National Research Centre, 12622, Giza, Egypt.
[d]Nutrition and Food ScienceDept., Faculty of Home Economics, Al-Azhar University, Egypt.

Abstract

The goal of this study was to compare the effects of kumquat extract and its chitosan nanoparticles on biochemical, histopathological, and parasitological factors in mice infected with *Toxoplasma gondii* versus spiramycin and control groups. A total of 35 mice, 7 of which were negative control and 28 was infected group, were used in the current study. All mice were sacrificed at 45 day after inoculation. Blood samples were collected. Then, sera Malondialdehyde (MDA), Catalase (CAT), Superoxide Dismutase 3 (SOD3), α-glutathione S-transferases (α-GST), and Interleukin 6 (IL-6) concentrations were measured using ELISA technique. In infected groups, CAT, SOD3, α-GST levels were decreased significantly (P<0.01), while MDA and IL-6 concentrations were significantly increased when compared to negative control (P<0.01). Treatment of infected mice with Kumquat-loaded chitosan nanoparticles were significantly improved (P<0.05) all parameters levels in sera and back them close to the original levels of negative control. The biochemical results are in parallel with histopathological and parasitological results. The findings imply that oxidative stress and parasitological changes may have a role in the aetiology and therapy of toxoplasmosis, particularly when Kumquat-loaded chitosan nanoparticles were used.
Key words: Toxoplasma gondii; Oxidative stress; Kumquat; Chitosan nanoparticles.

1. Introduction

Toxoplasma gondii, a worldwide protozoan parasite belonging to the Apicomplexa phylum, affects around 30% globally [1]. There are three stages to the parasite's life cycle. The sporozoite, which originates in the oocysts released by the definitive host, is a fast-propagating motile tachyzoite capable of infecting all nucleated cells, the metabolically active bradyzoite, and the metabolically active bradyzoite [2]. The infection which begins after the host cells are invaded by tachyzoites. It multiplies rapidly by endogenesis and then diffuses to colonize various tissues. Conversion into bradyzoites and synthesis of double membrane protective cysts permit parasite persistence in any infected host, just as tachyzoites are sensitive to host immune systems. They're typically found in skeletal muscle neurons and myocytes, as well as the heart. These cells appear to promote encystation and, more crucially, improve the likelihood of transmission by ingestion (myocytes) or are chemically appealing to neurons (tachyzoites) [3]. Septrin was employed as a reference medicine to treat toxoplasmosis and was given at doses of 100 and 200 mg/kg body weight, according to Harris's publication [4]. However, due to the emergence of drug-resistant parasites and dangerous types of side effects, this treatment regimen is not always suited for long-term use. As a result, new therapeutics are desperately needed [5,6].

Natural medicinal plants are increasingly being recognised for their therapeutic potential, which is typically considered less toxic and free of adverse effects than synthetic pharmaceuticals [7]. The Fortunella species (kumquat) is a citrus cousin from the Rutaceae family. Fresh kumquat fruits with skin can be eaten fresh whole [8,9,10]. Citrus fruits include polyphenols, vitamins, minerals, dietary fibres, essential oils, and carotenoids, making them a health-promoting fruit, according to past studies.

Citrus sinensis (sweet orange) and kumquat are the richest sources of phytochemicals that have been discovered as valuable pharmacological effects as cancer chemopreventive, anti-inflammatory, and neuroprotective candidates [11,12].

The nanoencapsulation of bioactive materials and pharmaceuticals utilising natural biopolymers has piqued interest in recent decades [13].

Natural biopolymers were improved biocompatibility of the compounds after encapsulation. Because of its biodegradability, biocompatibility, and low toxicity, chitosan is a suitable biopolymer for use as an encapsulating delivery method [14]. Chitosan is the second most abundant biopolymer on the planet. The most important source of chitosan is marine crustaceans [15]. More researchers have previously described chitosan as a carrier molecule that can be employed to boost the drug's effectiveness against various infections [16,17].

Chitosan is a naturally abundant and relatively inexpensive biopolymer with excellent biological features such as anticancer activity, antibacterial activity, and immunological boosting effects, which has piqued the interest of many researchers [18,19]. Nanoencapsulation of essential oils in chitosan is a new encapsulation method.

Infections can affect healthy hosts while also stimulating the immune system of the infected host. The immune system responds by producing harmful oxidants called free radical species [20]. Malondialdehyde (MDA), a reactive aldehyde that produces oxidative stress in tissue and cells, is formed when reactive oxygen species destroy polyunsaturated lipids [21]. MDA affects proteins by forming covalent adducts, which are thought to contribute to tissue damage [23].

Antioxidant defence mechanisms enable tissues to detoxify these hazardous oxidants, which are highly reactive chemical entities. All aerobic cells have superoxide dismutase (SOD) enzyme, an important antioxidant candidate. The antioxidant enzymes catalase (CAT) and glutathione peroxidase reduce superoxide to oxygen and hydrogen peroxide, which is then reduced to water by this enzyme [24,25]. CAT is a naturally occurring enzyme found in all living cells that protects them from oxidative harm by detoxifying hydrogen peroxide molecules and inhibiting the production of hydroxyl radicals [24].

Overall, the rationale of this study is to explore the changes of biochemical enzymes, oxidative stress markers, histopathological, and parasitological parameters in *Toxoplasma gondii* infected mice upon treatment with kumquat extract and kumquat loaded NPs compared to control groups.

2. Materials and Methods

Preparation of kumquat peel powder

Mature kumquat fruits (*Fortunella margarita*) were purchased from Ahmed Orabi Association, Al Obour, Egypt.

Kumquat fruits were washed under running water, dried, and hand peeled. Kumquat peel was spread on perforated stainless steel trays and dried in a shady and airy place at room temperature (30 ± 2°C) for 2 days. The dried orange peel was grinded to give consistent and fine powder using electrical grinder. The powdered kumquat peel was then stored in well labeled airtight container at refrigerator for further use.

Extraction of kumquat peel powder

Kumquat peel powder was extracted as described by Kadan's team [26] with some modifications. Two hundred grams of the kumquat peel powder were added to 800 ml of ethanol 90% in a beaker with magnetic stirrer and homogenized for 15 min at 60°C, then left in dark glass bottle for 24 h for complete extraction. The extract supernatant obtained was passed through a 0.2 μm filter and ethanol was evaporated using rotary evaporator.

Preparation of Kumquat chitosan nanocomposites

Preparation of nanoparticles (NPs) by ionotropic gelation method is based on electrostatic interaction between negatively- and positively-charged molecules such as poly anionic and cationic polymers. In the case of Kumquat-loaded chitosan NPs, the amino groups existed on chitosan links with anionic groups of tripolyphosphate (TPP) salt. Chitosan mixture was performed at 1 mg/mL in acidified distilled water (DW) and TPP was prepared at 1 mg/mL in DW. First, 1 mL of chitosan mixture was stirred for 10 min and its volume got attuned to 1.5 mL with DW. Next, added 5 μL tween 80 to 1 mg/mL of Kumquat extract. Then, Kumquat was added to the chitosan mixture. Finally, 100 μL of TPP solution as a cross linker were added to emulsified-Kumquat-chitosan solution in a dropwise way. The obtained solution was stirred for 30 min and centrifuged at 4000 g for 5 min. At last, the supernatant was transferred into a new tube and kept for subsequent analysis [27].

Kumquat-loaded chitosan NPs characterization

The samples were sonicated for 5 min before being analyzed and they were immediately used for measurements.

Entrapment efficiency measurement

Dialysis tubing technique was used to purify the synthesized NPs for eliminating the impurities and the free non-conjugated compounds suspended in the solution by eluting it through regenerated cellulose (Amicon 10,000 MWCO ultra filter, Millipore, USA). The Entrapment efficiency (EE%) for the NPs were measured and processed with the microplate reader (BMG Labtech, Germany). The compound entrapment efficiency was calculated from the ratio of the compound amount incorporated into the NPs to the total added compound amount [28].

Transmission electron microscopy (TEM)

Particle morphology of the NPs was examined by TEM (Philips CM-10, FEI Inc., Hillsboro, OR, USA). 100 μg/mL of the NPs were dropped into formvar-coated copper grids, and after complete drying, the samples were stained using 2% w/v uranyl acetate (Electron Microscopy Services, Ft. Washington, PA). Image capture and analysis was done using Digital Micrograph and Soft Imaging Viewer Software [29].

Particle size and zeta potential analyses

Particle size and zeta potential of the NPs were determined using Malvern Zeta Sizer (Nano ZS, Malvern Instruments, UK). All the samples were maintained at a constant temperature of 25.0°C.

Experimental design

Mice were purchased from Theodor Bilharz Research Institute, Imbaba—Giza, Stool examination of the mice was done prior to the study to sure the absence of any intestinal parasitic infection.

All animals (Swiss albino mice; n = 35; age 9–10 weeks; weight 20–25 g; all female). The mice were given drinking water and regular mouse food ad libitum. They were maintained according to the Ethics Committee of Theodor Bilharz Research Institute and in accordance with the "Guide for the care and use of laboratory animals" published by the US National Institutes of Laboratory Animal Resources.

The animals were divided equally into five groups (7 mice /cage) where they were categorized into the following groups; G1: non-infected and non-treated (negative control); GII: infected and non-treated (positive control); GIII: infected; treated with

Spiramycin; GIV: infected, treated with 0.1 ml of kumquat extract GV: infected and treated with 0.1 ml of kumquat extract-loaded chitosan (CS) nanoparticles (NPs), The infected mice were treated orally by using stomach tube either with Spiramycin at a dose of 200mg/kg daily starting first day post-infection (PI) for seven successive days (GIII) or with 0.1mg/kg of tested extracts (GIV and GV) twice daily for 14 successive days. All infected groups were received *T. gondii* cysts orally of the ME49 strain which obtained from Theodor Bilharz Research Institute, Imbaba, Giza (Fig 1).

At 45 day post-infection *T. Gondii* were counted in impression smears stained with Giemsa, from brain of infected mice. Where small pieces of all infected group brains were randomly selected and used to evaluate the parasitological changes. The brain weighed and macerated in 2 mL of sterile phosphate-buffered saline (PBS) using a tissue homogenizer. The cysts were counted using oil immersion and the mean of 10 different fields was calculated and then the mean was calculated for each group [30,31,32].
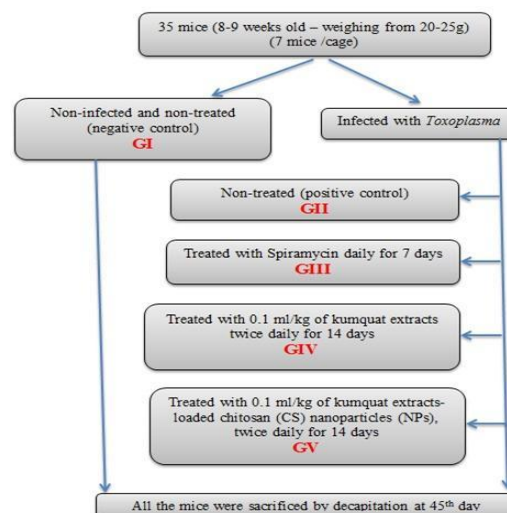

Fig. 1: Flow chart of experimental design

Estimation of the parasite count

The % reductions in the parasite counts were calculated according to the following equation:

$$\%R = \frac{100(C - E)}{C}$$

Where, R: reduction, C: control and E: experimental groups of mice [33].

Histopathological evaluation of brain

Specimens from the brain tissues of all studied groups were fixed in 10 % buffered formalin (pH 7.4) for 48 h. The tissue was dehydrated in an ethyl alcohol series, cleared in xylene and embedded in paraffin. The sections (5 μm) were de-waxed,

hydrated, and stained in Mayer's hemalum solution for 3 min. They were then stained with hematoxylin and eosin and prepared according to the method of Abdel-Wahab and his companions [34].

Biochemical measurements

Malondialdehyde (MDA), Catalase (CAT), Superoxide Dismutase 3 (SOD3), α-glutathione S-transferases (α-GST), and Interleukin 6 (IL-6) levels were measured using ELISA kits purchased from (Wuhan Fine Biotech Co., China).

Sample Collection and Storage

The whole blood sample was placed at room temperature for 2 hours and centrifuged for 20 minutes at approximately 1000×g. The serum was collected and the assay carried out immediately. The blood collection tubes were disposable, non-pyrogenic, and non-endotoxin.

Principle of ELISA measurements

These kits were based on Competitive-ELISA detection procedure. The provided microtiter plate has been pre-coated with target. During the reaction, target in the sample or standard competes with a fixed amount of target on the solid phase supporter for sites on the Biotinylated Detection Antibody specific to target. Excess conjugate and unbound sample or standard were washed from the plate, and *Streptavidin*-Biotin Complex (SABC) was added to each microplate well and incubated. Then 3,3′,5,5′-Tetramethylbenzidine (TMB) substrate solution is added to each well. The enzyme-substrate reaction is terminated and the color change is measured spectrophotometrically at a wavelength of 450nm. The concentration of target in the samples is then determined by comparing the OD of the samples to the standard curve.

Malondialdehyde (MDA)

Determination of lipid peroxidation levels

The levels of MDA, as a lipid peroxidation product, were determined using ELISA assay Kit (Wuhan Fine Biotech Co., China). In this method, the thiobarbituric acid (TBA) reactive substances (TBARS) quantity was detected as a MDA production index in serum samples based on nmol per ml of serum. The color change is measured spectrophotometrically at a wavelength of 450nm [35]

Catalase (CAT)

Determination of Catalase (CAT) enzyme activity was performed using ELISA assay Kit (Wuhan Fine Biotech Co., China). The assay was based on the reaction of catalase to decompose

hydrogen dioxide. According to the kit instructions, samples were mixed with buffer assay (hydrogen peroxide) and the reduction of absorbance as a result of hydrogen peroxidase elimination were recorded at a wavelength of 450nm [36]

Superoxide Dismutase 3 (SOD3)

Determination of SOD3 enzyme activity was performed using ELISA assay Kit (Wuhan Fine Biotech Co., China). Its activity in serum samples, as an important antioxidant enzyme, was recorded according to kit. In brief, after reduction of 2-(4-iodophenol)-3-(4-nitrophenol)-5-phenyltetrazolium chlo-ride by xanthine oxidase, a red formazan product was produced. This reduction was inhibited by SOD3 and the produced colored complex absorbance was quantified at 450nm.

α-glutathione S-transferases (α-GST)

Like GSH, it was determined through colorimetric method using 5, 5′-dithiobis-2-nitrobenzoic acid (DTNB) according to protocol provided by the kit. Briefly, DTNB reacted with reduced form of thiol (–SH) groups and makes complex. The absorbance was read at 450 nm to estimate the α-GST levels [37].

Interleukin 6 (IL-6)

This kit was based on sandwich enzyme-linked immune-sorbent assay technology. Determination of IL-6 levels was performed using ELISA assay Kit. The color change is measured spectrophotometrically at a wavelength of 450nm [38].

Statistical analysis

All results were presented as mean ± standard error (SE). Results were analyzed statistically by one-way analysis of variance (ANOVA) using SPSS 15.0 program, IBM Company (NY, USA) and value of $P<0.05$ was considered statistically significant.

3. Results

Characterization of the NPs

In the present study TEM used to illustrate the morphology of the synthesized kumquat NPs. Fig 2 showed the TEM image of the NPs and the sizes, ranging from 198 nm and 225.5 nm of the particles in the image. The image displays spherical NPs with a nano-capsule of CS shell.

The dialysis tubing approach was used to determine the entrapment efficiency (EE %) of synthesized kumquat NPs. The EE percent of the free

kumquat inside the nano-capsules was found to be 82.63 percent.

The Kumquat-loaded CS NPs were characterized using the Malvern Zeta Sizer equipment' Dynamic Light Scattering (DLS). Statistical analysis showed that their Z-average diameters were 205.45$\pm$ 7.23 nm. The polydispersity index (PDI) was 0.1, which reflects the high constancy of the kumquat NPs. On the surface of the Kumquat-loaded CS NPs, there was a constant pattern of positive charge (zeta potential) (ZP= + 17.5$\pm$3.41 mV).

The nano-formulation of the Kumquat-loaded CS NPs was very stable; where zeta potential and PDI index of the synthesized NPs indicated that they are stable formulations. Because the Zeta potential was not near to zero and the PDI value was less than 0.5, electrostatic stabilization would be sufficient to stabilize the systems.
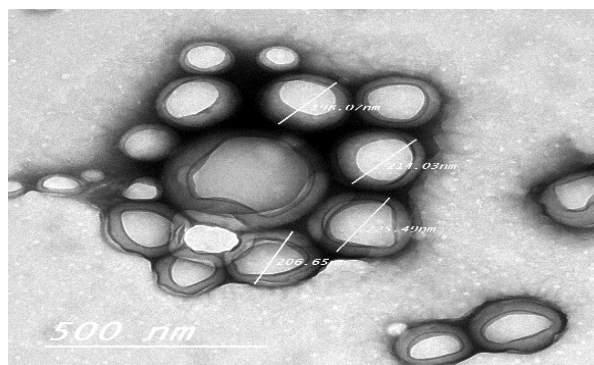

Fig. 2: TEM images of the Kumquat-loaded CS NPs. This image showed the morphology of the NPs. and illustrated the sizes, ranging from 198 nm and 225.5 nm of the particles of Kumquat-loaded CS.

Estimation of Toxoplasma cysts count in the brain

The brain was used as an index of the degree of *T. gondii* infection in this investigation. Fig 3 shows the average number of cysts in the mice brains with diagnosed chronic toxoplasmosis post- treatment with Kumquat extract and its NPs vs untreated control and spiramycin-treated drug.

Giemsa stained impression smears from the brains of animals revealed *T. gondii* tissue cysts. When animals treated with Kumquat-extract were compared to their matching control group, there was a statistically significant reduction in tissue cysts count in all tested groups (Fig. 3). This decrease in the mean tissue cyst count was observed to be more pronounced in group (GV) when compared to the other groups (GII and GIV).
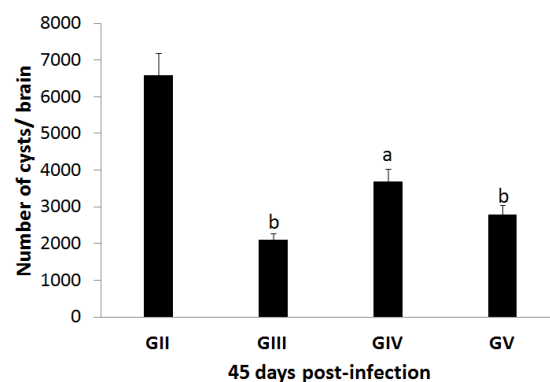

Fig. 3: Effect of treatments on tissue cysts number in brain at 45 days post-infection. a; means significance decrease (P < 0.05) when comparing GIV with GII. b; means high significance decrease (P < 0.01) when comparing GIII or GV with GII.

Biochemical measurements

ELISA technique was utilized to investigate some parameters in mice's sera. MDA, CAT, SOD3, GST, and IL6 levels were tested, and illustrated in Figs. 4. In infected group, CAT (Fig. 4A), SOD3 (Fig. 4B), α-GST (Fig. 4C) levels were decreased significantly (P <0.01), while MDA (Fig. 4A) and IL-6 (Fig. 4D) concentrations were significantly increased when compared to negative control (GI) (P<0.01).

Treatment of infected mice with Kumquat-loaded chitosan nanoparticles were significantly improved (P<0.05) all parameters levels in sera and back them close to the original levels of negative control. Indeed, the MDA and IL-6 levels in the treated mice with Spiramycin, Kumquat, and Kumquat NPs were significantly decreased (P<0.05) compared to the infected mice group (GII), reporting the highest significant decrease (P<0.01) using the Kumquat NPs.

On the other hand, the CAT, SOD3, α-GST concentrations in the treated mice with Spiramycin, Kumquat, and Kumquat-loaded chitosan nanoparticles showed significant decrease (P<0.05) compared to the infected mice group (GII), recording the highest significant decrease (P<0.01).

Histopathological changes

Figs 5-9 show histopathological changes in brain sections from different experimental groups H&E at high power view X (100 X, 200 X, and 400 X). Normal control group (G1) brain sections revealed average meninges, average cerebral cortex with average neurons, average striatum with average neurons and average glial cells, average pyramidal neurons in (CA1), (CA2), (CA3), and inter-neuron area, cerebellum with average molecular cell layer,

average Purkinje cell layer, average deep granular cell layer, and average medulla.
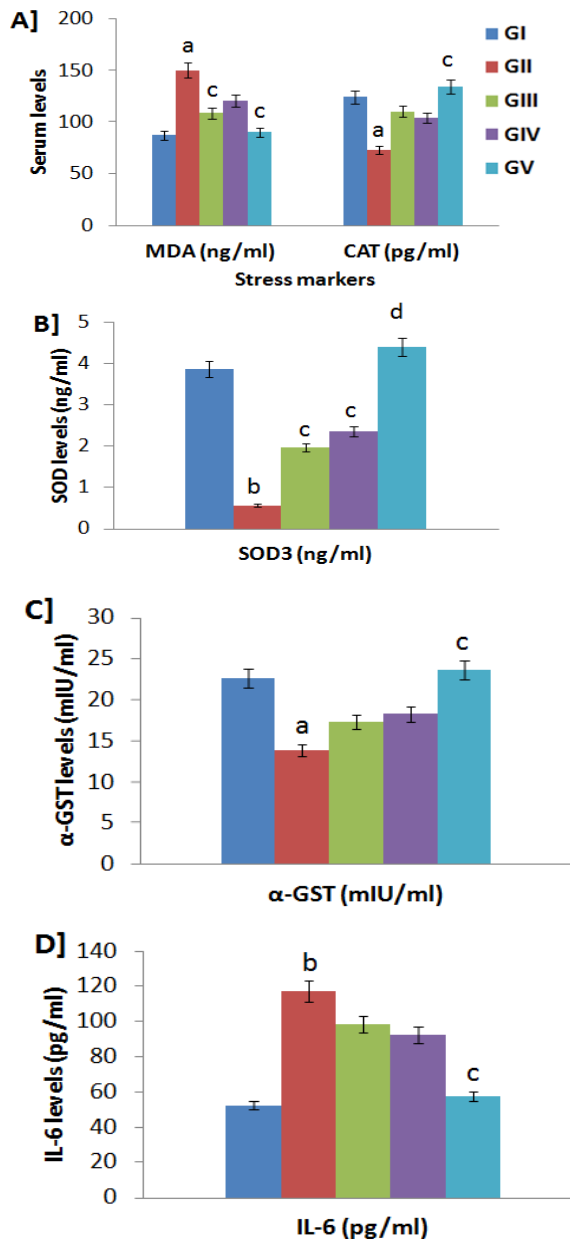

Fig. 4: MDA and CAT (A), SOD3 (B), α-GST (C), and IL-6 (D) sera levels upon treatments versus positive control (GII) and negative control (GI). a; means significance difference (P < 0.05) when comparing GII with GI. b; means high significance difference (P < 0.01) when comparing GII with GI. c; means significance difference (P < 0.05) when comparing treated groups with GII. d; means high significance difference (P < 0.01) when comparing treated groups with GII.
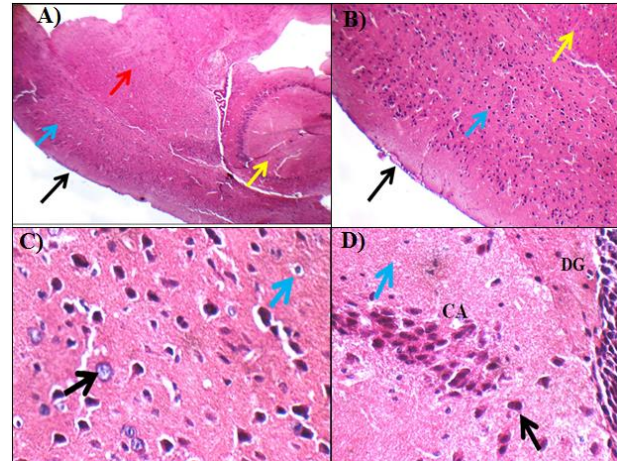

Fig 5: Normal control group (GI): A) brain showing average meninges (black arrow), average cerebral cortex (blue arrow), average striatum (red arrow), and average hippocampus (yellow arrow) (H&E X 100). B) high power view showing average meninges (black arrow), average cortex with average neurons (blue arrow), and average striatum (yellow arrow) (H&E X 200). C): another view in deep cortex showing average neurons (black arrow), and average glial cells (blue arrow) (H&E X 400). D) another view in hippocampus showing Cornu Amonis (CA3) with average pyramidal neurons (black arrow) and average inter-neuron area (red arrow), and average (DG) (H&E X 400).

Average meninges, hypercellular cerebral cortex with scattered degenerated neurons and few parasitic cysts, striatum with average neurons and few parasitic cysts, hippocampus with scattered degenerated pyramidal neurons in (CA1), (CA2), (CA3) and inter-neuron area, cerebellum with scattered degenerated neurons and parasitic cysts in medulla (Fig. 6).

Brain section of spiramycin treated group (GIII) showed average meninges, hypercellular cortex with scattered degenerated neurons in deep cortex, striatum with average neurons and average glial cells, hippocampus with few scattered degenerated pyramidal neurons in (CA1) and (CA2), cerebellum showed average molecular cell layer, average neurons in Purkinje cell layer, average deep granular cell layer, and average medulla (Fig. 7).
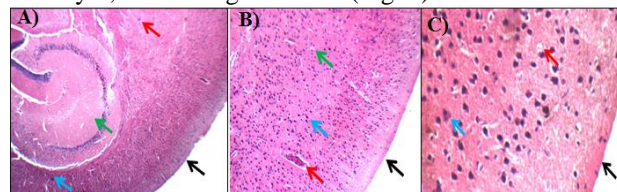

Fig 6: Control positive group (GII): A) brain showing average meninges (black arrow), parasitic cysts in cerebral cortex (blue arrow), and in striatum (red arrow), and average hippocampus (green arrow) (H&E X 100). B) high power view showing average meninges (black arrow), and hypercellular cerebral cortex showing parasitic cysts (green arrow), average neurons (blue arrow) and average blood vessels (red arrow) (H&E X 200). C) higher power view showing average meninges (black arrow), and cerebral cortex showing scattered degenerated neurons (blue arrow) and few parasitic cysts (red arrow) (H&E X 400).
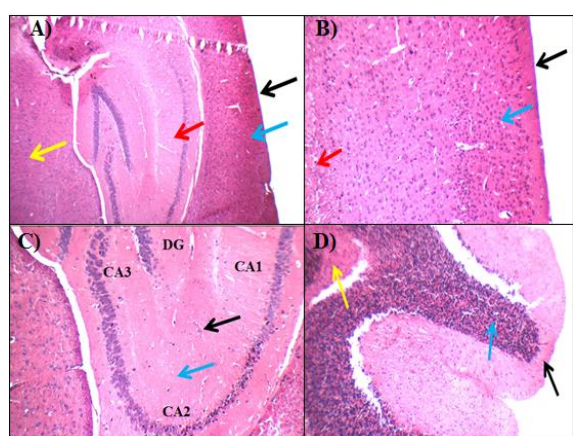
Fig 7: spiramycin-treated group (GIII): A) brain showing average meninges (black arrow), average cerebral cortex (blue arrow), average striatum (yellow arrow), and average hippocampus (red arrow) (H&E X 100). B) high power view showing average meninges (black arrow), hypercellular cortex with average neurons (blue arrow), and average striatum (red arrow) (H&E X 200). C)another view inhippocampus showing average Cornu Amonis (CA1), dentate gyrus (DG), average inter-neuron area (black arrow), and average blood vessels (blue arrow) (H&E X 200). D) another view in striatum showing markedly degenerated neurons (black arrow), and average glial cells (blue arrow) (H&E X 400).

Brain section of kumquat extract treated group (GIV) showed average meninges with mild sub-meningeal edema, cortex with markedly degenerated neurons and average glial cells, striatum with markedly degenerated neurons and average glial cells, hippocampus with markedly degenerated pyramidal neurons in (CA1), (CA2), and (CA3) and in inter-neuron area with parasitic cyst in (CA1), cerebellum showed average molecular cell layer, average neurons in Purkinje cell layer, average deep granular cell layer, and medulla showing scattered degenerated cells and mild small cyst formation (Fig. 8).

Brain section of kumquat extract loaded Chitosan nanoparticles treated group (GV) showed average meninges, hypercellular cortex with scattered degenerated neurons , striatum with markedly degenerated neurons, average glial cells and mild astrogliosis, hippocampus with degenerated pyramidal neurons in (CA1), (CA2), and (CA3) and in inter-neuron area, cerebellum showed thick meninges, average molecular cell layer, average neurons in Purkinje cell layer, average deep granular cell layer, and medulla showing dilated congested blood vessels, scattered degenerated cells, and marked inflammatory cellular infiltrate (Fig. 9).
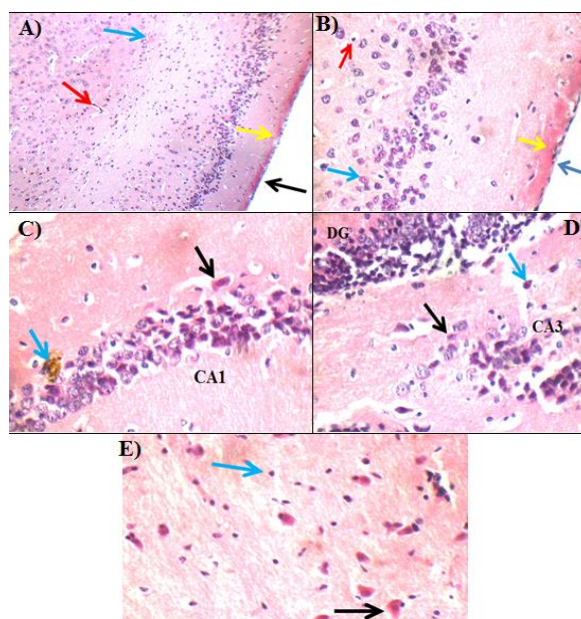

Fig 8: Kumquat extract treated group (GIV): A) brain showing average meninges (black arrow) with mild sub-meningeal edema (yellow arrow), hypercellular cortex with scattered degenerated neurons (blue arrow), and average blood vessels (red arrow) (H&E X 200). **B)** high power view showing average meninges (black arrow) with mild sub-meningeal edema (yellow arrow), hypercellular cortex with markedly degenerated neurons (blue arrow), and average glial cells (red arrow) (H&E X 400). **C)**high power view showing CornuAmonis (CA1) with scattered degenerated pyramidal neurons (black arrow), and parasitic cyst (blue arrow) (H&E X 400). **D)** another view inCornuAmonis (CA3) showing markedly degenerated pyramidal neurons (black arrow) and in inter-neuron area (red arrow), and average (DG) (H&E X 400). **E)** another view in striatum showing markedly degenerated neurons (black arrow), and average glial cells (blue arrow) (H&E X 400).
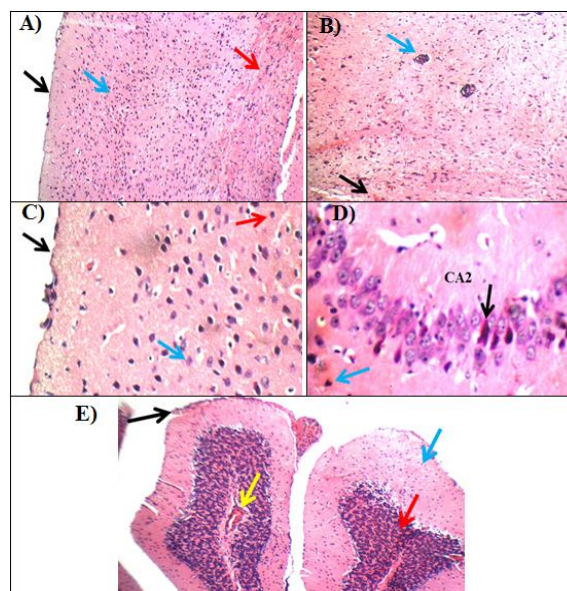

Fig 9: kumquat extract-loaded chitosan nanoparticles treated group (GV): A) brain showing average meninges (black arrow), hypercellular cortex with average neurons (blue arrow), and average striatum (red arrow) (H&E X 200). B) another view in

striatum showing scattered degenerated neurons (black arrow), and mild astrogliosis (blue arrow) (H&E X 200). C) high power view showing average meninges (black arrow), and hypercellular cortex with scattered degenerated neurons (blue arrow), and average glial cells (red arrow) (H&E X 400). D) another view in CornuAmonis (CA2) showing markedly degenerated pyramidal neurons (black arrow), and in inter-neuron area (blue arrow) (H&E X 400). E) cerebellum showing thick meninges (black arrow), cortex with average molecular layer (blue arrow),average deep granular cell layer (red arrow), and medulla showing dilated congested blood vessels (yellow arrow) (H&E X 200).

4. Discussion

This study was aimed to assess in vivo therapeutic effects of kumquat extract against chronic toxoplasmosis in mice. Since last centuries, plants and their derivatives have been used as a valuable natural resource for traditional remedies [39].

More than two-thirds of the global population trusts folk medicine for early therapeutic purposes, according to the World Health Organization (WHO) [40]. Many reviews demonstrated that herbs used for therapeutic purposes in traditional medicine contain a variety of compounds that have different biological and therapeutic activities especially in the treatment of microbial infections [41].

The antioxidant and antibacterial activity of various kumquat peel extracts led to the conclusion that the peel might be exploited as a natural bioactive source, particularly in the food and pharmaceutical industries [42,43].

The flavonoid concentration of citrus species, including our proposed drug, kumquat, is thought to be responsible for their antioxidant action [44]. Flavonoids have been linked to a reduction in the risk of developing certain chronic diseases [45]. Flavonoids have also been shown to have anti-cancer [46] and antiviral [47] properties. NPs can adjust pharmacokinetics, enhance bioavailability, and target release while posing modest toxicity risks [48]. The medicinal substance can be dissolved, absorbed, or encapsulated in the polymer matrix, making polymeric nanoparticles biocompatible and biodegradable.

They may include synthetic polymers such as polyethylene glycol (PEG), (poly (D,Llactic-co-glycolic acid) (PLGA), as well as natural ingredients like alginate, insulin, and chitosan (CS) [49]. CS is a polysaccharide that has been employed in medicine for the past two decades. It is a crucial substance for the manufacture of NPs since it is biodegradable and harmless [50]. As a result, it's employed as an antibiotic and antifungal [51]. Many researches on CS NPs have been conducted to determine their anti-parasitic activities; they provided minor protection in

the treatment of Giardia lamblia infection [52] and boosted the anti-filarial impact [53].

The goal of this study was to see how well kumquat-encapsulated CS NPs treated chronic toxoplasmosis infection in mice. The current study found that giving mice 0.1 ml/kg of kumquat extract for 14 days had substantial therapeutic effects against chronic toxoplasmosis. The findings imply that the decrease in parasite load in infected mice treated with Kumquat-loaded chitosan NPs can be linked to the strengthening of the immune system, particularly the innate immune system, which results in *T. gondii* infection control.

The efficiency of *Nigella sativa* aqueous extract and its CS NPs against Acanthamoeba keratitis was demonstrated in a previous study [54], and these agents show promise for the creation of innovative, effective, and safe treatments. A study performed by Aqeel's group [55] suggested a remarkable amoebicidal effect of the NPs. For the treatment of Cryptosporidium, Plasmodium falciparum, and Leishmania, CS NPs were employed as a drug delivery system [56,57,58]. The effectiveness of anti-Giardia compounds-loaded CS NPs was stated by Said's team [52].

In the present study, there was significant difference ($P < 0.05$) reduction in the average number of *T. gondii* cysts in mice brains treated with kumquat extract (GIV) and highly significant ($p < 0.01$) difference in GV compared with positive control group (GII).

The pathophysiology of toxoplasmosis is known to be related to the increased risk of oxidative stress in host cells due to the activation of inflammatory response against the parasite [59]. One of the critical host defence methods against intracellular parasites is oxidative stress generated by the immune system [60,61].

The antioxidant system, which includes both enzymatic and nonenzymatic antioxidants, works to protect the body from the damaging effects of reactive oxygen species [62].

According to previous study, on apicomplexan parasites,which showed that , catalase and superoxide dismutase (SOD) are the first enzymes that reacted directly with oxidants [63,64]. The decrease in SOD activity found in this study could be linked to the severity of parasitemia and oxidative stress increasing [65]. SOD is an important antioxidant that protects against oxygen radicals by dismuting superoxide radicals to H_2O_2, which can cause oxidative damage to lipids, proteins, and DNA [66,67]. SOD levels in the serum of Toxoplasma infected mice were found

to be lower. The main cause of decreased enzyme activity was considered to be an excessive accumulation of radicals in the tissue. Other studies in England and Turkey have found that the severity of toxoplasmosis, as well as a decrease in SOD activity in *T. gondii* infection, is the main source of oxidative stress [62,63].

In the present study, SOD was increased in the serum of *Toxoplasma* infected and treated with kumquat loaded CS NPs mice. The NPs can pass through capillaries and be absorbed by cells, allowing them to permeate tissues. Other research has discovered that chitosan derivative-based NPs can aid in the absorption of grape extracts [68,69] and, if internalised by enterocytes, can pass the intestinal epithelium unaltered and reach the blood, i.e. the target location.

More mucoadhesive NPs were found to be more effective at increasing the bioavailability of the encapsulated medication than those that were less mucoadhesive [69].

In the present study, CAT activity of serum was significantly reduced on day 45 in GII post infection. CAT action is unfavourably affected by oxidative stress produced upon toxoplasmosis infection [70]. There was high significant change in CAT activity in GV compared to GII at day 45 post infection. In Bahrami study [60], CAT activity of serum was significantly increased on day 45 post infection in group which treated with kumquat NPs. CS derivative-based NPs improve kumquat extract absorption, and Fabiano's group [69] demonstrated that once internalised by enterocytes, they can pass the intestinal epithelium and reach the blood, i.e., the target location. More mucoadhesive NPs were found to be more effective at increasing the bioavailability of the encapsulated medication than those that were less mucoadhesive [69]. *T. gondii* appears to have lowered the activity of ROS-encoding proteins.

Important enzymes like CAT and SOD lose their efficient function and become inactive as a result of the excessive synthesis of these active oxygen species [71]. The CAT enzyme minimises probable damage by detoxifying reactive oxygen species produced by immune cells [72].

In this study, there was a significant decrease in GSH levels in serum by day 45. Glutathione, a non-protein thiol source, can operate as a substrate for glutathione peroxidase and has been shown to be a functional protective molecule against oxidative damage in a variety of tissues [73]. Furthermore, decreasing serum GSH levels in chronic toxoplasmosis may alter the detoxification capability of particular tissues, resulting in tissue oxidation [74,75]. Increase GSH concentrations in serum in GV

treated with the NPs, which protected the antioxidants present in the drug from breakdown in the GI tract. Protected thiol groups in the NPs, on the other hand, have demonstrated to be more effective in the protection process from oxidative stress [76,77].

T. gondii infection dramatically increased lipid peroxidation, as measured by erythrocyte MDA values in this study. This could be due to an increase in the formation of free radicals and oxidants as a result of infection. Free radicals can cause genetic mutations or cytotoxicity when they react with DNA. They can also attach to polyunsaturated fatty acid-rich erythrocyte membranes [73], causing membrane breakdown and cellular damage [78].

MDA concentrations were increased dramatically in serum *Toxoplasma* infected mice GII, while there is no significant change between in GIII and GV in the present study. Karaman's team [74] stated that MDA levels were elevated in *T. gondii*-infected patients and mice. In chronic acquired toxoplasmosis, the level of MDA is elevated and can reflect indirectly the degree of oxidative cell damage. The findings of this investigation are consistent with [74], which revealed that *T. gondii* infection increased erythrocyte MDA concentrations considerably. The serum MDA concentrations of mice infected with *T. gondii*, on the other hand, did not change [79].

MDA was elevated as a result of this process, which created a cross link between membrane contents, particularly ion channels, resulting in an effect on membrane charges and enzyme activity [74]. MDA levels rose in the spleen, liver, and brain of *T. gondii*-infected mice [79]. Increase in MDA level as an essential lipid peroxidation marker was elevated in the study in Toxoplasma infected chickens, according to Al-team Kennany's [80].

In reality, after tissue damage, lipid peroxidation occurred in huge quantities, with MDA being the most prominent result of this process, leading to cell structure disruption, inflammation, and necrosis [81]. Authors [59,82,83] reported that MDA levels were significantly higher in asymptomatic *Toxoplasma* seropositive patients compared to healthy subjects. The NPs structure of CS was showed to be more effectual for ornamental extract uptake compared with free drug of Kumquat [84].

In present study, IL-6 cytokine was significantly increased at days 45 in GII post infection, IL-6 cytokine decreased in the treated groups (GIV and GV). Whereas kumquat loaded chitosan was more effective compared to the positive control (GII). IL-6 is an important citokine in the protective immune response against infectious agents such as *T. gondii* [85,86,87].

Studies on mice treated with RH for 7 days after infection indicated an increase in cytokines such as INF-γ, TNF-α, and IgM against parasitic tachyzoites using spiramycin-loaded chitosan nanoparticles [88]. The immune system of mice treated with kumquat-loaded chitosan NPs improved and was enhanced, according to the findings of this study.

T. gondii regulation in the central nervous system is mostly mediated by cytokines. Microglia triggered by cytokines are essential host-defining cells in infections of the central nervous system. According to new research, cytokines can also activate astrocytes, causing them to suppress intracellular infections.

The cytokines IFN-γ, TNF-α, IL-1, and IL-6 are known to have a role in regulating T. gondii replication in the brain. The ability of cytokines to activate astrocytes and suppress T. gondii replication may also play a role in the reactivation of Toxoplasma infections in AIDS [89].

Most of therapeutic agents are ineffective against brain tissue cysts due to their impaired metabolism and blood-brain barrier resistance [90]. The predominance of a persistent infection may have a role in the development of a number of neurological and neurobehavioral problems [91]. Toxoplasma favors neuronal cells over resident glial cells in the CNS, where it differentiates into encysted bradyzoites and establishes a latent or chronic infection. However, as infection progressed, astrocytes and microglia were able to successfully limit the parasites' proliferation and multiplication. After that, bradyzoite-containing vacuoles were usually discovered in neurons [92].

In the present research, histopathological examination of brain sections from infected mice revealed variable degrees of perivascular, interstitial inflammatory infiltrates, astrocytosis, degenerated neurons and meningitis. Also our findings showed few parasitic cysts, striatum with average neurons and few parasitic cysts with scattered degenerated neurons and parasitic cysts in medulla.

These findings support prior research [93,94] that demonstrated T. gondii infection triggers a robust cellular immune response.

Brain slices of infected untreated mice exhibited Toxoplasma cysts surrounded by chronic inflammatory cells in Toxoplasma ME49 strain affected subgroups.

El-team Temsahy's team [95] also made similar observations. Etewa's group [96] showed that Infected mice had neurobehavioral problems.

Variable degrees of perivascular and interstitial inflammatory infiltrates, astrocytosis, deteriorated neurons, and meningitis were demonstrated by histopathology when compared to uninfected controls.

In group (GIII), after administration of spiramycin, resolution of pathological changes was noticed besides degeneration of the existing cysts. On the other hand, in group (GIV), after treatment with kumquat loaded-chitosan nanoparticles treated group (GV), the degree of inflammatory infiltration increased. Similar results were demonstrated by Scharton-Kersten's group [97] who found that in chronically infected mice with T. gondii, inducible nitric oxide synthase (iNOS) inhibitor L-NMMA (N^G-Methyl-L-arginine, acetate salt) showed reactivation of infection with increased inflammatory changes in brain tissues. In contrast to previous observation, it was observed that the control of intra-cerebral persisting toxoplasmosis in the latent phase of the toxoplasma infection [98].

The tissue structure of the organs studied changed in the group of rats infected with T. gondii ME49 but not treated. Curcumin and curcumin NPs treatment enhanced the histomorphology of infected rats, which could be attributed to curcumin's anti-inflammatory properties [99].

Etewa's team [100] showed a marked improvement of the pathological pictures of brain, liver, spleen and eye in the subgroup received spiramycin-loaded chitosan NPs. He illustrated that encapsulating of spiramycin on CS NPs raised its antiparasitic impact on the infection of T. gondii infection.

Histopathological studies revealed that groups treated with drugs loaded on CS NPs contained no hydatid cysts with improvement in the degree of inflammation, necrosis, and congestion of hepatic tissue [101].

Conclusion

The findings of the current study imply that biochemical, oxidative stress, and parasitological changes may have a role in the aetiology and therapy of toxoplasmosis in mice, particularly when Kumquat-loaded chitosan NPs are applied.

- Competing of Interests:
The authors declare that there is no conflict of interest.

-Authors Contributions:
AA Abd-Rabou, the corresponding author, synthesized and characterized the nanoparticles. All authors (WF Abd El-Hamed, AA Abd-Rabou, NS Yousef, ZA Salem) contributed in all biological experiments in this work; mice

modelling, parasitology, and histopathology, biochemical, stress markers, and ELISA sections, as well as writing and editing the manuscript.

References

1. Spalenka, J., Hubert, J., Voutquenne-Nazabadioko, L., Escotte-Binet, S., Borie, N., Velard, F., Villena, I., Aubert, D., Renault, J. H. (2020). *In Vitro* and *In Vivo* Activity of *Anogeissus leiocarpa* Bark extract and isolated metabolites against *Toxoplasma gondii*.Planta Medica, 86 (4): 294–302.

2. Halonen, S.K. & Weiss, L.M. (2013). Toxoplasmosis. Handb. Clin. Neurol., 114, 125–145.

3. Mendez, O.A. & Koshy, A.A. (2017). *Toxoplasma gondii*: Entry, association, and physiological influence on the central nervous system. PLoS Pathogens., 13, e1006351. https://doi.org/10.1371/journal.ppat.1006351

4. Harris, C., Salgo, M.P., Tanowitz, H.B. & Wittner, M. (1988). *In vitro* assessment of antimicrobial agents against *Toxoplasma gondii*. J. Infect. Dis., 1570: 14–22.

5. Djurkovic, O., Milenkovic, V., Nikolic, A., Bobic, B. & Grujic, J. (2002). Efficacy of atovaquone combined with clindamycin against murine infection with a cystogenic (Me49) strain of *Toxoplasma gondii*. J. Antimicrob. Chemother., 50: 981-987.

6. Ferreira, R., Oliveira, A.B., Ribeiro, M.F., Tafuri, W.L., Vitor, R.W. (2006).*Toxoplasma gondii*: *In vitro* and *in vivo* activities of the hydroxyl-naphthoquinone 2-hydroxy-3-(1-propen-3-phenyl)-1, 4-naphthoquinone alone or combined with sulphadiazine. Exp. Parasitol., 113:125-129.

7. Abu-El-Ezz, N.M. (2005). Effect of *Nigella sativa* and *Allium cepaoils* on *Trichinella spiralis*in experimentally infected rats. J. Egypt Soc. Parasitol., 35: 511-523.

8. Kumamoto, H., Matsubara, Y., Irzuka, Y., Okamoto, K. & Yokoi, K. (1985).Structure and hypotensive effect of flavonoid glycosides in kinkan (*Fortunella japonica*) peelings. Agric. Biol. Chem. 49: 2613–2618.

9. Ogawa, K., Kawasaki, A., Omura, M., Yoshida, T., Ikoma, Y. & Yano, M. (2001). 3′5′-Di-C-β-glucopyranosyl phloretin, a flavonoid characteristic of the genus *Fortunella*. Phytochemistry, 57: 737–742.

10. El-Shafae, A. & Ibrahim, M. (2003). Bioactive kauranediterpenes and coumarins from *Fortunella margarita*. Pharmazie, 58:143–144.

11. Genovese, S., Fiorito, S., Locatelli, M., Carlucci, G., & Epifano, F. (2014). Analysis of biologically active oxyprenylated ferulic acid derivatives in citrus fruits. Plant Foods for Human Nutrition, 69 (3): 255-260.

12. Sadek, E.S., Makris, D.P. & Kefalas, P. (2009). Polyphenolic composition and antioxidant characteristics of kumquat (*Fortunella margarita*) peel fractions. Plant Foods for Human Nutrition, 64(4): 297-302.

13. Cui, H., Bai, M., Marwan, M.A., Rashed M.M.A. & Lin, L. (2018).The antibacterial activity of clove oil/chitosan nanoparticles embedded gelatin nanofibers against *Escherichia coli* O157:H7 biofilms on cucumber. Int. J. Food Microb. 266, 69–78.

14. Hadidi, M., Pouramin, S., Adinepour, F., Haghani, S. & MahdiJafari, S. (2020).Chitosan nanoparticles loaded with clove essential oil: Characterization, antioxidant and antibacterial activities. Carbohyd. Polym. 236, https://doi.org/10.1016/j.carbpol.2020.116075

15. Zhang, H., Liang, Y., Li, X. & Kang, H. (2020). Effect of chitosan-gelatin coating containing nano-encapsulated tarragon essential oil on the preservation of pork slices. Meat Sci. 166, 108137. DOI: 10.1016/j.meatsci.2020.108137

16. Ma, Z. & Lim, L.Y. (2003). Uptake of chitosan and associated insulin in Caco-2 cell monolayers: a comparison between chitosan molecules and chitosan nanoparticles. Pharm Res., 20 (11):1812-1819.

17. Ma, Z., Lim, T.M. & Lim, L.Y. (2005). Pharmacological activity of peroral chitosan–insulin nanoparticles in diabetic rats. Int. J. Pharm., 293 (1-2): 271-280.

18. Gu, H., Ho, P.L., Tong, E., Wang, L. & Xu, B. (2003). Presenting vancomycin on nanoparticles to enhance antimicrobial activities. Nano Lett., 3: 1261-1263.

19. Dutta P.K., Rinki, K. & Dutta, J. (2011). Chitosan: A Promising Biomaterial for Tissue Engineering Scaffolds, Eds.: R. Jayakumar, M. Prabaharan and R.A.A. Muzzarelli), Springer Berlin Heidelberg, Berlin, Heidelberg, 45-79.

20. Saleh, M.A., Mahran, O.M., Al-Salahy M.B. (2011).Circulating oxidative stress status in dromedary camels infested with sarcoptic mange. Vet. Res.Commun, 35, 35-45.

21. Pryor, W.A. & Stanley, J.P. (1975).Letter: A suggested mechanism for the production of malonaldehyde during the antoxidation of polyunsaturated fatty acids. None enzymatic production of prostaglandin endoperoxides during antioxidation. J. Org. Chem., 40, 3615-3617.

22. Farmer, E.E. & Davoine, C. (2007). Reactive electrophile species. Curr.Opin. Plant Biol., 10, 380-386.

23. Traverso, N., Menini, S., Maineri, E.P., Patriarca, S., Odetti, P., Cottalasso, D., Marinari, U.M., Pronzato, M.A. (2004). Malondialdehyde, a lipoperoxidation-derived aldehyde, can bring about secondary oxidative damage to proteins The Journals of Gerontology Series A: Biological Sciences and Medical Sciences., 59 (9): 890–895.

24. Akkus, I. (1995). Serbest radikaller ve fizyopatolojik etkileri. 1-151. Mimoza Basım Yayım ve Dağıtım A.S. Konya.

25. Halliwell, B. & Chirico, S. (1993).Lipid peroxidation: its mechanism, measurement, and significance Am J Clin Nutr, 57, 715-725.

26. Kadan, S., Rayan, M., & Rayan, A. (2013). Anticancer activity of anise (*Pimpinella anisum* L.) seed extract. The Open Nutraceuticals Journal, 6 (1).1-5. **DOI:** 10.2174/1876396001306010001

27. Desai, K.G. (2016) Chitosan nanoparticles prepared by ionotropic gelation: An overview of recent advances. Crit Rev Ther Drug Carrier Syst.; 33 (2):107-158.

28. Abd-Rabou, A.A, & Ahmed, H.H. (2017). CS-PEG decorated PLGA nano-prototype for delivery of bioactive compounds: A novel approach for induction of apoptosis in HepG2 cell line. Advances in Medical Sciences 62: 357–367.

29. Abd-Rabou, A.A., Abdelaziz, A. M., Shaker, O.G., & Ayeldeen, G. (2021). Metformin-loaded lecithin nanoparticles induce colorectal cancercytotoxicity via epigenetic modulation of noncoding RNAs. MolBiol Rep., In Press, doi: 10.1007/s11033-021-06680-8.

30. Araujo, F.G., Prokocimer, P., Lin, T.E.R.I., & Remington, J.S. (1992). Activity of clarithromycin alone or in combination with other drugs for treatment of murine toxoplasmosis. Antimicrobial Agents and Chemotherapy, 36 (11): 2454-2457.

31. Thiptara, A., Kongkaew, W., Bilmad, U., Bhumibhamon, T., & Anan, S. (2006). Toxoplasmosis in piglets. Annals of the New York Academy of Sciences, 1081 (1), 336-338.

32. Barakat, A.M.A. (2007). Some diagnostic studies on male New Zealand rabbit experimentally infected with *Toxoplasma gondii* strain. Global veterinaria, 1(1), 17-23.

33. Penido, M.L.D.O., Nelson, D.L., Vieira, L.Q., & Coelho, P.M.Z. (1994). Schistosomicidal activity of alkyl amino octane thio sulfuric acids. Memórias do Instituto Oswaldo Cruz, 89, 595-602.

34. Abdel-Wahab, M. F., Esmat, G., Milad, M., Abdel-Razek, S., & Strickland, G. T. (1989). Characteristic sonographic pattern of schistosomal hepatic fibrosis. The American Journal of Tropical Medicine and Hygiene, 40 (1): 72-76.

35. Zhang, H., Fan, L., Liao, H., Tu, L., Zhang, J., Xu, D., & Feng, J. (2021) Correlations of cardiac function with inflammation, oxidative stress and anemia in patients with uremia. *ExpTher Med.,* 21: 250 https://doi.org/10.3892/etm.2021.9681.

36. Jackson, M.I., Waldy, C., & Jewell, D.E. (2020). Dietary resistant starch preserved through mild extrusion of grain

alters fecal microbiome metabolism of dietary macronutrients while increasing immunoglobulin A in the cat. PLoS One, 15 (11): e0241037. https://doi.org/10.1371/journal.pone.0241037

37. Esmaeilzadeh-Gharehdaghi, E., Razmara, E., Bitaraf, A., Jamshidi, A., Mahmoudi, M., & Garshasbi, M. (2020) Functional analysis of RELN S2486G mutation and its contribution to pathogenesis of Ankylosing Spondylitis. *Arch. Iran Med.,* 23 (10):688-696.

38. Wang, T., Li, Z., Xia, S., Xu, Z., Chen, X., & Sun, H. (2021). The protective effects of Ramelteon against isoflurane-induced insults and inflammatory response in brain microvascular endothelial cells. *Neurotox Res.,* 39: 677-686.

39. Rocha, L.G, Almeida, J.R., Macedo, R.O., Barbosa-Filho, J.M. (2005). A review of natural products with antileishmanial activity. Phytomedicine ; 12: 514-35.

40. World Health Organization. (2019). WHO Global Report on Traditional and Complementary Medicine. https://apps.who.int/iris/handle/10665/312342

41. Anand, U., Jacobo-Herrera, N., Altemimi, A., & Lakhssassi, N. (2019). A comprehensive review on medicinal plants as antimicrobial therapeutics: potential avenues of biocompatible drug discovery. Metabolites, 9 (11), 258. DOI:10.3390/metabo9110258

42. Al-Saman, M.A., Abdella, A., Mazrou, K.E., Tayel, A.A. & Irmak, S. (2019). Antimicrobial and antioxidant activities of different extracts of the peel of kumquat (*Citrus japonica* Thunb).Journal of Food Measurement and Characterization, 13(4), 3221-3229.

43. Figueiredo, C., Barroso, J., Pedro, L., Scheefeer, J. (2007) Factors affecting secondary metabolite production in plants: volatile components and essential oils. Flavour Fragr. J. 22, 206–213.

44. Roowi, S., & Crozier, A (2011). Flavonoids in tropical citrus species. J. Agric. Food Chem. 59 (22), 12217–12225

45. Lefevre, M., Beecher, G.R., Gross, M.D., Keen, C.L., & Etherton, T.D. (2004). Bioactive compounds in nutrition and health -research methodologies for establishing biological function: the antioxidant and anti-inflammatory effects of flavonoids on atherosclerosis. Annu. Rev. Nutr. 24, 511–538.

46. Taylor, P., Nichenametla, S.N., Taruscio, T.G., Barney, D.L., & Exon, J.H. (2006) A review of the efects and mechanisms of polyphenolics in cancer. Crit. Rev. Food Sci. Nutr. 46(2), 161–183

47. Asres, K., Seyoum, A., Veeresham, C., Bucar, F., & Gibbons, S. (2005). Naturally derived anti-HIV agents. Phytother. Res. 19 (7): 557–581.

48. Khalil, N.M., de Mattos, A.C., Carraro, T.C, Ludwig, D.B. & Mainardes, R.M. (2013). Nanotechnological strategies for the treatment of neglected diseases. Curr Pharm Des., 19 (41): 7316–7329.

49. Chan, J.M., Valencia, P.M., Zhang, L., Langer, R., & Farokhzad, O.C. (2010). Polymeric nanoparticles for drug delivery. In: Cancer Nanotechnology, (Eds.) S.R. Grobmyer, B.M. Moudgil (pp. 163-175). Humana Press. DOI 10.1007/978-1-60761-609-2_11

50. Ing, L.Y., Zin, M.N., Sarwaran, A. & Katas, H. (2012). Antifungal activity of chitosan nanoparticles and correlation with their physical properties. Int J Biomater, Volume 2012, Artecle ID: 632698. https://doi.org/10.1155/2012/632698

51. Kean, T., & Thanou, M. (2010). Biodegradation, biodistribution and toxicity of chitosan. Advanced drug delivery reviews, 62 (1): 3-11.

52. Said, D.E., Elsamad, L.M., & Gohar, Y.M. (2012). Validity of silver, chitosan, and curcumin nanoparticles as anti-Giardia agents. Parasitology research, 111(2), 545-554.

53. Ali, M., Afzal, M., Verma, M., Misra-Bhattacharya, S., Ahmad, F.J., & Dinda, A.K. (2013). Improved antifilarial activity of ivermectin in chitosan–alginate nanoparticles

against human lymphatic filarial parasite, Brugia. malayi. Parasitology Research, 112 (8), 2933-2943.

54. Elkadery, A.A.S., Elsherif, E.A., Eldin, H.M.E., Fahmy, I.A.F. & Mohammad, O.S. (2019). Efficient therapeutic effect of *Nigella sativa* aqueous extract and chitosan nanoparticles against experimentally induced *Acanthamoeba keratitis*. Parasitology research, 118 (8), 2443-2454.

55. Aqeel, Y., Siddiqui, R., Anwar, A., Shah, M.R., Khoja, S. & Khan, N.A. (2015). Photochemotherapeutic strategy against Acanthamoeba infections. Antimicrob Agents Chemother 59 (6): 3031–3041.

56. Kayser, O. (2001). A new approach for targeting to *Cryptosporidium parvum* using mucoadhesive nanosuspensions: research and applications. International journal of pharmaceutics, 214(1-2), 83-85.

57. Föger, F., Noonpakdee, W., Loretz, B., Joojuntr, S., Salvenmoser, W., Thaler, M., & Bernkop-Schnürch, A. (2006). Inhibition of malarial topoisomerase II in *Plasmodium falciparum* by antisense nanoparticles. International journal of pharmaceutics, 319 (1-2): 139-146.

58. Pujals, G., Suñé-Negre, J. M., Pérez, P., García, E., Portus, M., Tico, J.R. & Carrió, J. (2008). *In vitro* evaluation of the effectiveness and cytotoxicity of meglumine antimoniate microspheres produced by spray drying against *Leishmania infantum*. Parasitology research, 102 (6), 1243-1247.

59. Al-Kuraishy, H.M., Al-Kuraishi, A.H., Al-Windy, S. & Al-Gareeb, A.I. (2020). Toxoplasmosis and risk of endothelial dysfunction: Role of Oxidative Stress and Pro-Inflammatory Mediators . Arch. Clin. Infect. Dis., 14, 6–11.

60. Bahrami, S., Shahriari, A., Tavalla, M., Azadmanesh, S., & Hamidinejat, H. (2016). Blood Levels of Oxidant/Antioxidant Parameters in Rats Infected with *Toxoplasma gondii*. Oxidative Med. Cell. Longev.; 1–6. doi: 10.1155/2016/8045969.

61. Motavalli, M., Khodadadi, I., Fallah, M. & Maghsood, A.H. (2018): Effect of oxidative stress on vital indicators of *Acanthamoeba castellanii* (T4 genotype). Parasitol Res.; 117(9):2957-2962.

62. Atmaca, N., Cinar, M., Güner, B., Kabakci, R., Gazyagci, A.N., Atmaca, H.T., & Canpolat, S., (2015). Evaluation of oxidative stress, hematological and biochemical parameters during *Toxoplasma gondii* infection in gerbils. Ankara Üniv Vet FakDerg.; 62: 165–170.

63. Bosch, S.S, Kronenberger, T., Meissner, K.A., Zimbres, F.M., Stegehake, D., Izui, N.M., Schettert, I., Liebau, E., Wrenger, C., (2015). Oxidative stress control by apicomplexan parasites. Biomed Res Int.; 2015:ID:351289 https://doi.org/10.1155/2015/351289

64. AbdEllah, M.R., (2013). Involvement of free radicals in parasitic infestations. J Appl. Anim Res.; 41 (1): 69–76.

65. Rezaei, S.A., & Dalir-Naghadeh, B. (2006). Evaluation of antioxidant status and oxidative stress in cattle naturally infected with *Theileria annulata*. Veterinary parasitology, 142(1-2), 179-186.

66. Alscher, R.G., Erturk, N. & Heath, L.S. (2002). Role of superoxide dismutases (SODs) in controlling oxidative stress in plants. Journal of experimental botany, 53(372), 1331-1341.

67. Alajmi, R.A., AL-Megrin, W.A., Metwally, D., Al-Subaie, H., Altamrah, N., Barakat, A. M., & El-Khadragy, M (2019). Anti-*Toxoplasma* activity of silver nanoparticles green synthesized with *Phoenix dactylifera* and *Ziziphus spina*-christi extracts which inhibits inflammation through liver regulation of cytokines in Balb/c mice. Biosci Rep.; 39 (5): https://doi.org/10.1042/BSR20190379.

68. Felice, F., Zambito, Y., Belardinelli, E., D'Onofrio, C., Fabiano, A., Balbarini, A., & Di Stefano, R. (2013). Delivery of natural polyphenols by polymeric nanoparticles improves the resistance of endothelial progenitor cells to oxidative stress. European Journal of Pharmaceutical Sciences, 50 (3-4), 393-399.

69. Fabiano, A., Piras, A.M., Uccello-Barretta, G., Balzano, F., Cesari, A., Testai, L., Citi, V. & Zambito, Y. (2018). Impact of mucoadhesive polymeric nanoparticulate systems on oral bioavailability of a macromolecular model drug. Eur. J. Pharm. Biopharm., 130, 281–289.

70. Kwok, L.Y., Schlüter, D., Clayton, C. & Soldati, D. (2004). The antioxidant systems in *Toxoplasma gondii* and the role of cytosolic catalase in defense against oxidative injury. Mol. Microbiol.; 51 (1): 47–61.

71. Dincel, G.C. & Atmaca, H.T.. (2016). Role of oxidative stress in the pathophysiology of *Toxoplasma gondii* infection. Int J Immuno pathol Pharmacol.; 29 (2): 226–240.

72. Kim, J.H., Lee, J., Bae, S.J.,Kim, Y., Park, B., Choi, J, Kown, J., Cha, G., Yoo, H.J., Jo, E.K., Bae, Y.S., Lee, Y.H. & Yuk, J.M. (2017). NADPH oxidase 4 is required for the generation of macrophage migration inhibitory factor and host defense against *Toxoplasma gondii* infection. Sci Rep.; 7(1):6361.DOI:10.1038/s41598-017-06610-4.

73. Nagalakshmi, N. & Prasad, M. (2001). Responses of glutathione cycle enzymes and glutathione metabolism to copper stress in *Scenedesmus bijugatus*. Plant Sci.; 160 (2): 291–299.

74. Karaman, U., Celik, T., Kıran, T.R., Colak, C. & Daldal, N.U. (2008). Malondialdehyde, glutathione, and nitric oxide levels in *Toxoplasma gondii* seropositive patients. Korean J Parasitol, 46, 293-295.

75. Jafari, M., Salehi, M., Shirbazou, S., Abasian, L. & Talebi-Meymand, F. (2014). Evaluation of gender-related differences in response to oxidative stress in *Toxoplasma gondii* positive serum. Annals of Military & Health Sciences Research; 12 (2): 64–69.

76. Beconcini, D., Fabiano, A., Zambito, Y., Berni, R., Santoni, T., Piras, A.M., & Di Stefano, R. (2018). Chitosan-based nanoparticles containing cherry extract from *Prunus avium* L. to improve the resistance of endothelial cells to oxidative stress. Nutrients, 10 (11), 1598. DOI:10.3390/nu10111598

77. Fisher, C.J. (2003): Lipid hydroperoxide (LOOH) of the fatty acid (FA) nature. Free Rad Biol Med, 77, 1-11.

78. Gilbert, H.S., Stump, D.D. & Roth, E.F. (1984): A method to correct for errors caused by generation of interfering compounds during erythrocyte lipid peroxidation. Anal. Biochem, 137, 282- 286.

79. Engin, A.B., Dogruman-Al, F., Ercin, U., Celebi, B., Babur, C., & Bukan, N. (2012). Oxidative stress and tryptophan degradation pattern of acute *Toxoplasma gondii* infection in mice. Parasitology research, 111(4), 1725-1730.

80. Al-Kennany E.(2007). Pathological study on the capability of *Toxoplasma gondii* to induce oxidative stress and initiation a primary lesion of atherosclerosis experimentally in broiler chickens. J Anim Vet Adv.; 6:938–942.

81. Zhang, H.b., Shen, Q.K., Wang, H, Jin, C., Jin, C.M. & Quan, Z.S. (2018). Synthesis and evaluation of novel arctigenin derivatives as potential anti-*Toxoplasma gondii* agents. Eur J Med Chem.; 158: 414–427.

82. Kiran, T.; Karaman, U.; Arici, Y. & Yildiz, S. (2019). Comparison of malondialdehyde, nitric oxide, adenosine deaminase and glutathione levels in patients with *Entamoeba coli*, *Enterobius vermicularis*, *Giardia intestinalis*, *Demodex* spp. positive, hydatid cyst and *Toxoplasma gondii* serum positive. Ann. Med. Res., 26 (7): 1420-1425.

83. Yazar, S., Kilic, E., Saraymen, R., & Sahin, I. (2003). Serum malondialdehyde levels in *Toxoplasma* seropositive patients. Annals of Saudi medicine. https://doi.org/10.5144/0256-4947.2003.413

84. Bowman, K. & Leong, K.W. (2006). Chitosan nanoparticles for oral drug and gene delivery. Int. J. Nanomedicine, (1):117-128

85. Jebbari, H., Roberts, C.W., Ferguson, D.J., Bluethmann, H., & Alexander, J. (1998).A protective role for IL-6 during early infection with *Toxoplasma gondii*.Parasite immunology, 20 (5), 231-239.

86. Mirpuri, J., & Yarovinsky, F. (2012).IL-6 signaling SOCS critical for IL-12 host response to *Toxoplasma gondii*. Future Microbiol.7, 13–16. DOI: 10.2217/fmb.11.147

87. Castro, A.S., Alves, C.M., Angeloni, M.B., Gomes, A.O., Barbosa, B.F., Franco, P.S., Silva, D.A.O., Martins-Filho, O.A., Mineo, J.R. & Ferro, E.A.V. (2013). Trophoblast cells are able to regulate monocyte activity to control *Toxoplasma gondii* infection. Placenta, 34, 240–247.

88. Hamad, H.K., Ramadan, N.F., Mohamed S.H., Aly, I.R., Zalat, R.S. (2018). Parasitological and immunological study of the effect of chitosan and chitosan nanoparticles loaded with spiramycin on toxoplasmosis. J. Global. Pharm. Technol.; 10 (6):138–145.

89. Klein, S.A., Dobmeyer, J.M., Dobmeyer, T.S, Pape, M., Ottmann, O.G., Helm. E.B., Hoelzer, D. & Rossol, R. (1997). Demonstration of the Th1 to Th2 cytokine shift during the course of HIV-1 infection using cytoplasmic cytokine detection on single cell level by flow cytometry. AIDS.; 11: 1111–1118.

90. Schultz, T.L., Hencken, C.P., Woodard, L.E., Posner, G.H., Yolken, R.H., Jones-Brando, L., & Carruthers, V.B. (2014). A thiazole derivative of artemisinin moderately reduces Toxoplasma gondii cyst burden in infected mice. J Parasitol., 100: 516–521.

91. Sinai AP, Watts EA, Dhara A, Murphy RD, Gentry MS, Patwardhan A. Reexamining chronic Toxoplasma gondii infection: surprising activity for a "dormant" parasite. Curr Clin Microbiol Rep 2016; 3(4):175-185.

92. . Lüder CG, Giraldo-Velásquez M, Sendtner M, Gross U. Toxoplasma gondii in primary rat CNS cells: Differential contribution of neurons, astrocytes, and microglial cells for the intracerebral development and stage differentiation. Exp Parasitol 1999; 93 (1): 23-32.

93. Mady, R.F., El-Hadidy, W., Elachy, S. (2016). Effect of *Nigella sativa* oil on experimental toxoplasmosis. Parasitol Res., 115: 379–390.

94. Chen, J., Huang, S.Y., Zhou, D.H., Li, Z.Y., Petersen, E., Song, H.Q., Zhu, X.Q. (2013) DNA immunization with eukaryotic initiation factor-2a of *Toxoplasma gondii* induces protective immunity against acute and chronic toxoplasmosis in mice. Vaccine 31 (52): 6225–6231.

95. El-Temsahy, M.M., El-Kerdany, E.D., Eissa, M.M., Shalaby, T.I., Talaat, I.M., Mogahed, N.M. (2016). The effect of chitosan nanospheres on the immunogenicity of *Toxoplasma lysate* vaccine in mice. J Parasit Dis., 40 (3): 611–626.

96. Etewa, S.E, Sarhan, M.H., , H.S.F., Mohammad, S.M, Samir, M.A., Kandil, A.M., Mostafa, E.M. (2021). Behavior and neuropsychiatric changes in experimental chronic toxoplasmosis: Histopathological and immunohistochemical studies. Parasitologists United Journal, 14, (2): DOI: 10.21608/puj.2021.75319.1120

97. Scharton-Kersten, T., Yap, G., Magram, J., Sher A. (1997). Inducible nitric oxide is essential for host control of persistent but not acute infection with the intracellular pathogen *Toxoplasma gondii*. J Exp Med., 185 (7):1261-1273.

98. Kroncke K, Fehsel K, Kolb-Bachofen V. Inducible nitric oxide synthase in human diseases. Clin. Exp. Immunol., 113 (2):147-156.

99. El-Shafey, A.A.M., Hegab, M.H.A., Seliem, M.M.E., Baraka, A.M.A., Mostafa, N.E., Maksoud, H.A.A. and Abdelhameed, R.M. (2020). Curcumin@metal organic frameworks nano-composite for treatment of chronic toxoplasmosis. Journal of Materials Science: Materials in Medicine, 31: 90. https://doi.org/10.1007/s10856-020-06429-y

100. Etewa, S.E., Abo El-Maaty, Rania S. Hamza, R.S., Metwaly, A.S., Sarhan, M.A., Abdel-Rahman, S.A., Fathy, G.M., El-

Shafey, M.A.(2018) Assessment of spiramycin-loaded chitosan nanoparticles treatment on acute and chronic toxoplasmosis in mice. J Parasit Dis., 42(1):102–113.

101. Kishik, S.M., Nagati, I.M., Ali, I.R., Aly, N.S.M., Fawzy, M.M. & Ali, H.S. (2021). Pathological assessment of *Nigella sativa* oil and its chitosan loaded nanoparticles on experimental hepatic cystic echinoncoccosis. DOI: 10.21608/puj.2021.59854.1105.